Iranian Journal of Medical Physics

ijmp.mums.ac.ir

Calculation of Temperature Rise in Multi-layer Biological Tissue Based on Large Aperture Concave Sphere Focused Ultrasonic Transducer

Hu Dong[1*], Gang Liu[1,2], Gaofeng Peng[1], Zhenzhong Ma[1]

1. School of Information Science and Engineering, Changsha Normal University, Changsha 410100, China
2. School of Physics and Electronics, Central South University, Changsha 410083, China

A R T I C L E I N F O

Article type:
Original Paper

Article history:
Received: March 13, 2022
Accepted: Jun 21, 2022

Keywords:
Simulation Model
High-Intensity Focused Ultrasound
Intensity of Sound
Nonlinear

A B S T R A C T

Introduction: The large aperture concave spherical focused ultrasonic transducer has stronger acoustic focusing effect and can obtain good temperature rise effect. The purpose of this study was to explore the effect of different frequency, duty cycle and inner radius parameters on temperature rise of multi-layer biological tissue.

Material and Methods: The simulation model of high-intensity focused ultrasound (HIFU) irradiated multi-layer biological tissue was constructed. By changing the irradiation frequency, duty cycle and inner radius of large aperture concave spherical focused ultrasonic transducer, the sound field and temperature field of multi-layer biological tissue were simulated and calculated by using Westervelt nonlinear acoustic wave equation and Pennes biological heat conduction equation, respectively.

Results: The intensity of sound field increased with the increase of frequency, while it decreased with the increase of inner radius, but the duty cycle almost had no effect on the intensity of sound field. The focal temperature increased with the increase of frequency and duty cycle, but decreased with the increase of inner radius.

Conclusion: By selecting appropriate parameters of transducer, the optimum temperature rise in the target area of biological tissue can be obtained by using a large aperture concave spherical focused ultrasonic transducer.

► *Please cite this article as:*
Dong H, Liu G, Peng G, Ma Zh. Calculation of Temperature Rise in Multi-layer Biological Tissue Based on Large Aperture Concave Sphere Focused Ultrasonic Transducer . Iran J Med Phys 2023; 20: 64-71. 10.22038/IJMP.2022.64394.2103.

Introduction

Biomedical ultrasound refers to the research of ultrasound in the fields of biology and medicine, which includes ultrasound diagnosis and ultrasound treatment, and it has the characteristics of non-invasiveness and high efficiency. High-intensity focused ultrasound (HIFU) is the most typical therapeutic ultrasound in biomedical ultrasound. It can not only be used to treat cancer, but also be applied in many other fields, such as hemostasis, ultrasonic lithotripsy, and cardiac conduction [1-3]. Thermal effect is the most important biological effect of HIFU in the treatment of tumor tissue.The principle of this technology is to use a wide caliber focused ultrasonic transducer to concentrate the acoustic wave energy in the focus area, and make the temperature reach the high temperature above 65 °C in a short time, resulting in irreversible degeneration and necrosis of cellular proteins and loss of active function, which will lead to the thermal coagulation and necrosis of the target tissue, and then achieve the purpose of killing cancer cells. In the histological examination of the focus treated by HIFU, there is often a narrow boundary between living cells and necrotic cells due to the obvious difference in the temperature gradient between the focus area and the surrounding tissue area. In recent years, the sound field and temperature field of focused ultrasound has been widely studied by many researchers. For example, Yuldashev et al. used the Khokhlov-Zabolotskaya-Kuznetsov (KZK) equation to study the propagation of finite amplitude sound beam in multi-layer biological tissue [4]. Zhao et al. used KZK equation to calculate the sound field in turbid water [5]. Fan et al. used the spherical beam equation (SBE) model to calculate the sound field in the oblate spheroidal coordinates [6], and Dong et al. calculated the sound field in biological tissue by SBE equation and analyzed the temperature field caused by focused ultrasound [7]. Haddadi et al. used Westervelt equation to calculate the temperature field through a focused ultrasonic transducer with wide aperture angle and compared it with the experimental data [8].

As a potential cancer treatment program, HIFU has been widely researched for many years. However, some problems still need to be solved. Because of high heating rate of HIFU, the acoustic focal position shift is

*Corresponding Author: Tel: +86-0731-84036108; Email: wjd3203@163.com

difficult to control, which limits its development and application. In order to monitor the HIFU treatment process in real time and improve its treatment efficiency, a ring-focused ultrasound transducer with B-mode probe in the center can be used. Kujawska et al. designed a ring-shaped transducer to concentrate acoustic energy on heat necrosis site [9]. The sound field was calculated by using Rayleigh integral, and then the temperature field was calculated by using Pennes equation [10]. They studied the relationship between the size and shape of the heat necrosis area and the radiation dose, which was determined by sound intensity and radiation duration.

In this paper, the temperature field generated by large aperture concave spherical focused ultrasonic transducer in five-layer media is analyzed. Firstly, the sound field generated by large aperture concave spherical focused ultrasonic transducer is calculated by Westervelt equation and the thermal deposition is obtained. Then, by solving the Pennes bioheat equation, the temperature field distribution in five-layer media is obtained, including the changes of several parameters related to the obtained temperature field are analyzed.

Materials and Methods

Theory

The KZK equation is used to calculate the sound field of ultrasonic transducer based on parabolic approximation, so it is only applicable to the transducer with half aperture angle less than 16° (half of the aperture angle of transducer) [11]. The large aperture focused ultrasonic transducer is a spherical shell focused transducer with half angle greater than 16°. Compared to small aperture focused transducer, large aperture focused transducer has stronger acoustic focusing effect and smaller focus area radius. Because of these characteristics, focal area exhibits higher temperature elevation, while other area exhibit lower temperature elevation. The large aperture focused transducer can be modeled by Westervelt equation. Figure 1 shows our numerical simulation model, where r_2 is the geometric outer radius of the radiation surface of the ultrasonic transducer, r_1 is the geometric inner radius of the radiation surface of the transducer, F is the focusing distance of the transducer, d_1 is the propagation distance of ultrasound in water, d_2 is the thickness of skin, d_3 is the thickness of fat, d_4 is the thickness of muscle, d_5 is the thickness of liver. The simulation model of multi-layer biological tissue irradiated by HIFU is shown in figure 1.

.

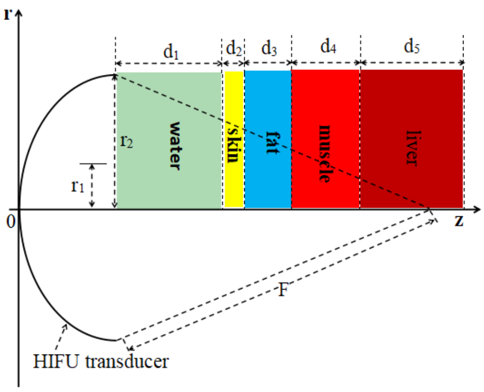

Figure 1. Simulation model of multi-layer biological tissue irradiated by HIFU

Figure 1 shows the simulation model of multi-layer biological tissue. The parameters used in the simulation are r_1 = 1.0 cm, r_2= 3.0 cm, F= 5.0 cm, d_1= 2.0 cm, d_2= 0.2 cm, d_3= 0.8 cm, d_4= 1.0 cm, d_5= 2cm, the irradiation frequency of ultrasonic transducer is 1MHz. The initial surface sound pressure of transducer is 0.24 Mpa, which can usually be measured with a needle hydrophone [12].

In order to describe the absorption, diffraction, and nonlinear effects of ultrasonic propagation in thermally viscous media, the widely used Westervelt wave equation is adopted, which can be written as follow [13]:

$$\left(\nabla^2 - \frac{1}{c_0^2}\frac{\partial^2}{\partial t^2}\right)p + \frac{\delta}{c_0^4}\frac{\partial^3 p}{\partial t^3} + \frac{\beta}{\rho c_0^4}\frac{\partial^2 p^2}{\partial t^2} = 0 \quad (1)$$

Where ∇^2, p, c_0, t are Laplace operator, sound pressure, sound velocity and time, respectively. $\beta = 1 + (B/2A)$ is the nonlinear coefficients, and B/A is the ratio of the second-order (B) coefficients to the first-order (A) coefficients of the Taylor series expansion [14]. $\delta = 2\alpha c_0^3/\omega^2$ is acoustic diffusivity which considers thermal viscosity effect in media, where ω is acoustic angular frequency and α is sound absorption coefficient. When the irradiation frequency is f, the corresponding sound absorption coefficient can be expressed as follow [15]:

$$\alpha(f) = \alpha_*(f/f_*)^{\mu} \quad (2)$$

Where α_* is the sound absorption coefficient of media with acoustic frequency f_*. The index μ is generally taken as 2 in water and 1.14 in biological tissue. The sound intensity of sound wave is I, the sound absorption coefficient of media is α, and the heat accumulation can be expressed as [16]:

$$Q_v = 2\alpha I \quad (3)$$

The Pennes equation can be expressed as [17]:

$$\rho_0 c_t \frac{\partial T}{\partial \tau_h} = K_t \nabla^2 T - \omega_b c_b (T - T_b) + Q_m + Q_v \tag{4}$$

Where ρ_0 is the density, c_t is the specific heat capacity of the media, τ_h is the heating time, K_t is the heat conduction coefficient of the media, T is the temperature of the media, ω_b is the blood flow rate when heating in the heating area, c_b is the specific heat capacity of the blood, T_b is the blood temperature of the heating area, Q_m is the heat generation rate of the media. Suppose that before heating, the temperature distribution at each point of the media is uniform and the temperature is T_0, the blood flow rate is ω_{b0}, and there is heat exchange between blood and media due to temperature difference. The heat exchange capacity per unit time and unit volume is equal to the heat generation rate of the media [18]:

$$Q_m = \omega_{b0} c_b (T_0 - T_b) \tag{5}$$

When the temperature rise of $T' = T - T_0$ is introduced, the heat produced by biological metabolism can be ignored for the tissue in vitro, and Q_m can be ignored, the heat generation rate of the space heat source Q_v is the only energy source, and the Pennes equation is written as [19]:

$$\rho_0 c_t \frac{\partial T'}{\partial \tau_h} = K_t \nabla^2 T' + Q_v \tag{6}$$

In the elliptic coordinate system, the Hamiltonian operator is expanded as follow:

$$\nabla \to \frac{1}{h_1 h_2 h_3}\left[\frac{\partial}{\partial \sigma}\left(\frac{h_2 h_3}{h_1}\frac{\partial}{\partial \sigma}\right) + \frac{\partial}{\partial \eta}\left(\frac{h_1 h_3}{h_2}\frac{\partial}{\partial \eta}\right) + \frac{\partial}{\partial \varphi}\left(\frac{h_1 h_2}{h_3}\frac{\partial}{\partial \varphi}\right)\right] \tag{7}$$

Where $h_1 = b\sqrt{\frac{\sigma^2+\eta^2}{1+\sigma^2}}$, $h_2 = b\sqrt{\frac{\sigma^2+\eta^2}{1\text{-}\eta^2}}$, $h_3 = b\sqrt{(\sigma^2+\eta^2)(1-\eta^2)}$ are the *Lame* coefficients of coordinate transformation, substituting them into the above equation can be simplified as follow:

$$\frac{dT'}{d\tau_h} = \frac{K_t}{b^2(\sigma^2+\cos^2\theta)\rho c_t} \times \left[2\sigma\frac{\partial T'}{\partial \sigma} + (1+\sigma^2)\frac{\partial^2 T'}{\partial \sigma^2} + ctg\theta\frac{\partial T'}{\partial \theta} + \frac{\partial^2 T'}{\partial \theta^2}\right] + \frac{Q_v}{\rho_0 c_t} \tag{8}$$

Where b and θ are the length of focal point of ellipsoidal coordinate system, the included angle between the projection of any point in the coordinate system and the focal line on the x-z plane and the x axis, respectively. $\sigma = z/b\eta$, $\eta = \cos\theta$, and z is the distance from the focus to the source point of ultrasonic transducer.

By using Crank-Nicolson implicit difference dispersion method [20], the following equation can be obtained.

$$\begin{Bmatrix} -(1+\frac{K_t}{2}\cot\theta)\sum_2 T'^{m+1}_{r,s} + (1+\frac{K_t}{2}\cot\theta)\sum_2 T'^{m+1}_{r,s+1} \\ (1-\frac{K_t}{2}\cot\theta)\sum_2 T'^{m+1}_{r,s-1} - 2\sum_2 T'^{m+1}_{r,s} + (1+\frac{K_t}{2}\cot\theta)\sum_2 T'^{m+1}_{r,s+1} \\ (1-\frac{K_t}{2}\cot\theta)\sum_2 T'^{m+1}_{r,s-1} + (\frac{K_t}{2}\cot\theta - 1)\sum_2 T'^{m+1}_{r,s} \end{Bmatrix} \cdot \begin{Bmatrix} s=1 \\ s=2, s\max-1 \\ s=s\max \end{Bmatrix} =$$

$$[\sigma H\sum_1 - (1+\sigma^2)\sum_1]T'^{m}_{r-1,s} + [2(1+\sigma^2)\sum_1 T'^{m}_{r,s}] - [\sigma H\sum_1 + (1+\sigma^2)\sum_1]T'^{m}_{r+1,s} - (\sigma^2+\cos^2\theta)\tau_h Q_v/\rho c_t$$

$$\sum_1 = \frac{K_t \tau_h}{b^2 \rho_0 c_t H^2}, \quad \sum_2 = \frac{K_t \tau_h}{b^2 \rho_0 c_t K^2} \tag{9}$$

Table 1. Acoustic and thermal parameters of media (1 MHz) [18,22-24]

Parameters	Media				
	water	skin	fat	muscle	liver
ρ_0 (kg.m^{-3})	1000	1090	910	1090	1050
c_0 (m.s^{-1})	1500	1530	1430	1550	1050
α (Np.m^{-1}.MHz^{-1})	0.025	11.53	9.0	23	4.5
β	3.5	4.5	10.5	4.5	6.0
μ	2.0	2.0	1.14	1.14	1.14
c_t (J.K^{-1}.kg^{-1})	4180	3300	3700	3600	3700
K_t (W.m^{-1}.K^{-1})	0.5	0.45	0.5	0.42	0.5

The temperature rise distribution at the focus is obtained by solving the above equation (9) with the pursuit method [21].

Simulation parameters

The sound field and temperature field of large aperture concave spherical focused ultrasonic transducer were simulated by using the software of MATLAB 2018b (MathWorks, Natick, Massachusetts, United States). The acoustic and thermal parameters of relevant media were given in Table 1.

Results

Sound field simulation

Figure 2 showed the simulation result of sound intensity under different frequency, duty cycle and inner radius, respectively, and the sound intensity had a direct effect on focal temperature field. The duty cycle was calculated as follow [25]:

$$duty\ \text{cycle}(\%) = \frac{t_{on}}{t_{on}+t_{off}} \times 100\% \tag{10}$$

Where t_{on} is the pulse duration (seconds) and t_{off} is the pulse interval (seconds). The number of pulse repetitions ($t_{on}+t_{off}$) corresponds to the number of cycles within the extraction time. In this work, the extraction time depended on the number of pulse repetitions and varied with each duty cycle.

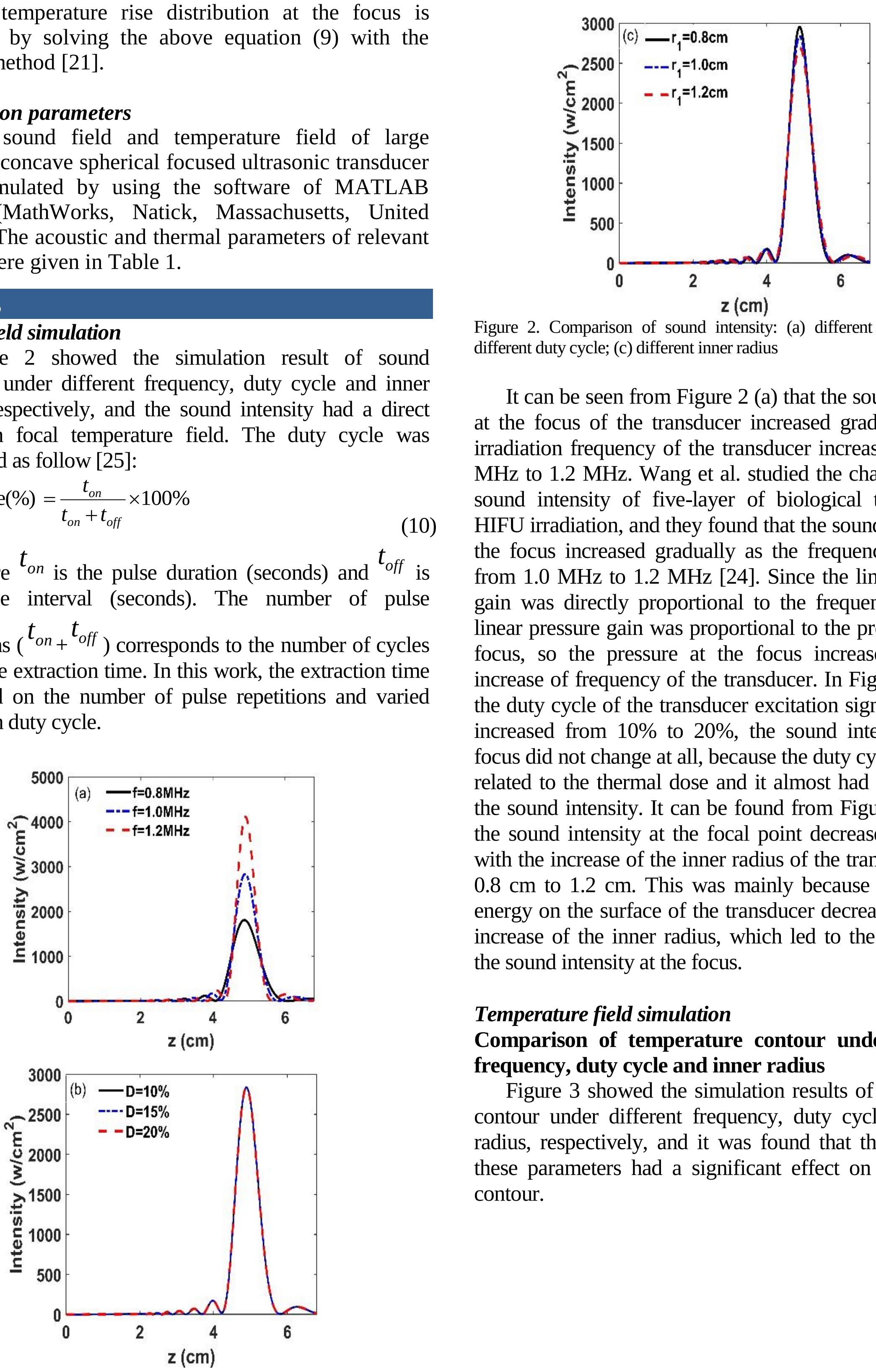

Figure 2. Comparison of sound intensity: (a) different frequency; (b) different duty cycle; (c) different inner radius

It can be seen from Figure 2 (a) that the sound intensity at the focus of the transducer increased gradually as the irradiation frequency of the transducer increased from 0.8 MHz to 1.2 MHz. Wang et al. studied the change of axial sound intensity of five-layer of biological tissue under HIFU irradiation, and they found that the sound intensity at the focus increased gradually as the frequency increased from 1.0 MHz to 1.2 MHz [24]. Since the linear pressure gain was directly proportional to the frequency, and the linear pressure gain was proportional to the pressure at the focus, so the pressure at the focus increased with the increase of frequency of the transducer. In Figure 2 (b), as the duty cycle of the transducer excitation signal gradually increased from 10% to 20%, the sound intensity at the focus did not change at all, because the duty cycle was only related to the thermal dose and it almost had no effect on the sound intensity. It can be found from Figure 2 (c) that the sound intensity at the focal point decreased gradually with the increase of the inner radius of the transducer from 0.8 cm to 1.2 cm. This was mainly because the acoustic energy on the surface of the transducer decreased with the increase of the inner radius, which led to the decrease of the sound intensity at the focus.

Temperature field simulation

Comparison of temperature contour under different frequency, duty cycle and inner radius

Figure 3 showed the simulation results of temperature contour under different frequency, duty cycle and inner radius, respectively, and it was found that the change of these parameters had a significant effect on temperature contour.

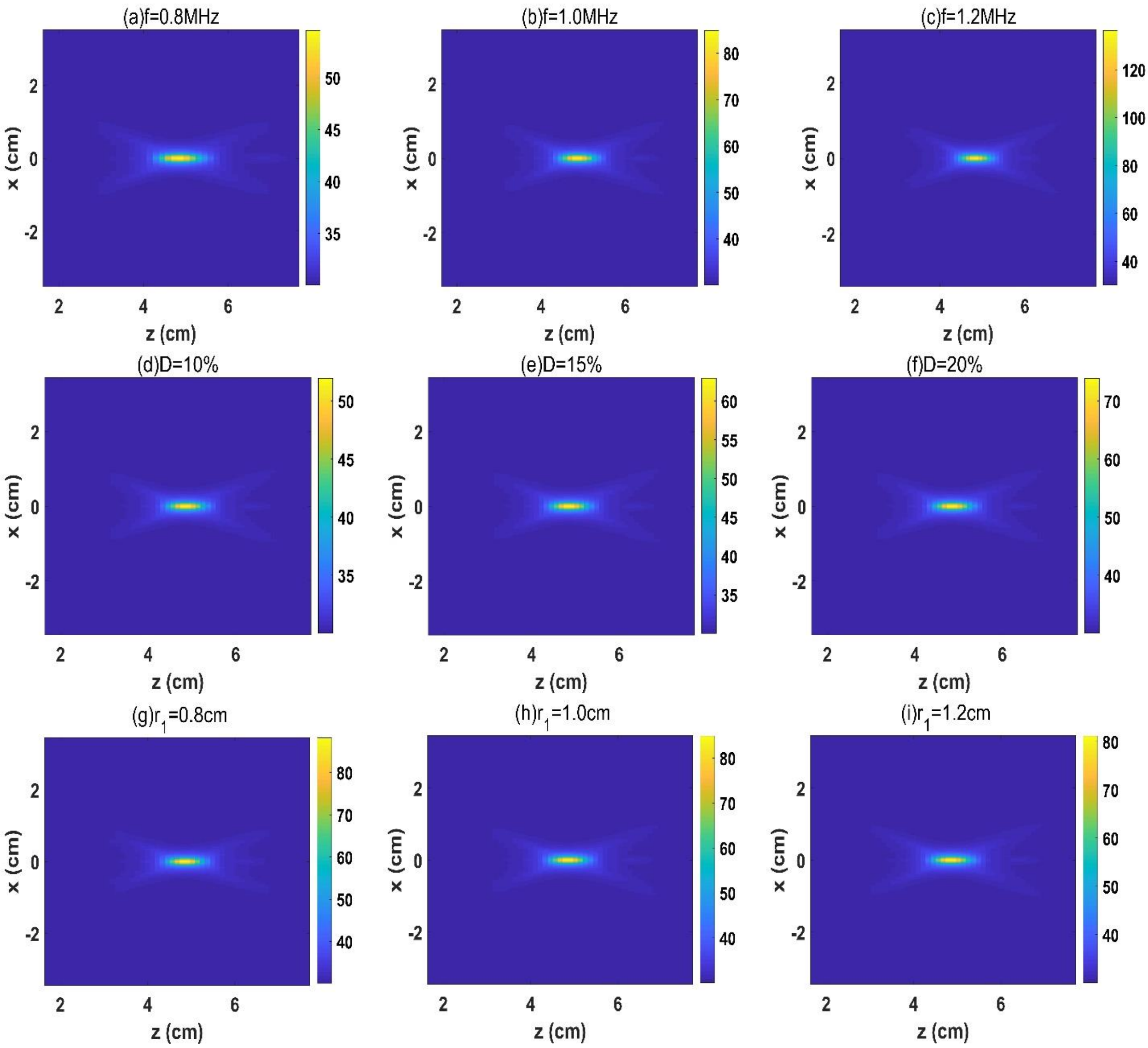

Figure 3. Comparison of temperature contour: a-c different frequency; d-f different duty cycle; g-i different inner radius

In order to analyze the influence of different frequency, duty cycle and inner radius parameters on the temperature field, Figure 3 showed the simulation results of temperature contour corresponding to five-layer of media. Under a certain sound pressure of sound source, it can be seen from Figure 3 a-c that with the increase of transducer frequency, the heat affected zone was gradually reduced, and the acoustic energy was more concentrated in the focus zone. The reason for this was that the absorption coefficient was closely related to the frequency of the sound source. Therefore, more acoustic energy was dissipated, leading to higher temperature rise. Because of the second harmonic generation, this effect was very prominent in the focus area. In Figure 3 d-f, with the duty cycle of excitation signal gradually increasing from 10% to 20%, the heat affected zone was gradually reduced, and the acoustic energy was more concentrated in focal region. It can be seen from Figure 3 g-i that with the increase of the inner radius of the transducer from 0.8 cm to 1.2 cm, the heat affected zone gradually increased and the acoustic energy was more divergent in focal region.

Comparison of focal temperature rise under different frequency, duty cycle and inner radius

Figure 4 showed the simulation results of focal temperature rise at different frequency, duty cycle and inner radius, respectively.

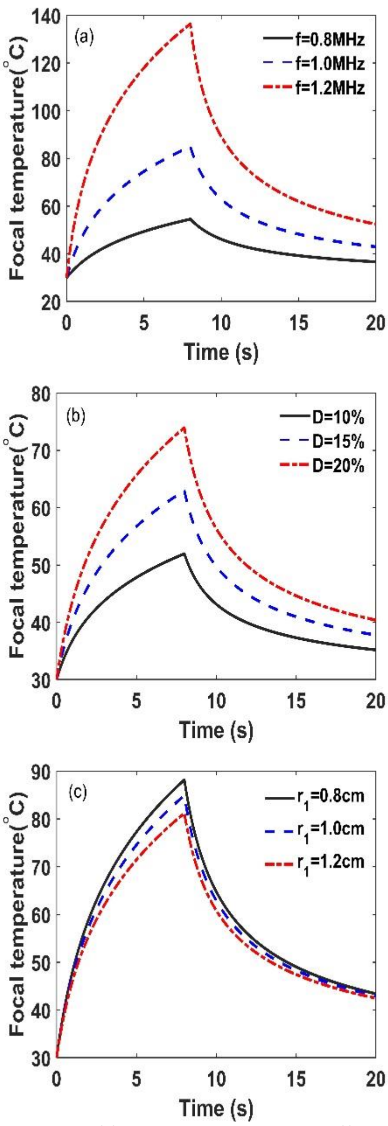

Figure 4. Comparison of focal temperature rise: (a) different frequency; (b) different duty cycle; (c) different inner radius

It can be seen from Figure 4 that the temperature of focal region of biological tissue increased first and then decreased whether changing the irradiation frequency and duty cycle of ultrasound or changing the inner radius of the transducer. Figure 4 (a) showed that the focal temperature increased with the increase of transducer frequency from 0.8 MHz to 1.2 MHz. Similarly, Gupta et al. also found that in multi-layer biological tissue, with the increase of irradiation frequency from 0.8 MHz to 1.2 MHz, the focal temperature also increased correspondingly [23]. It can be seen from Figure 4 (b) that as the duty cycle of the transducer excitation signal gradually increased from 10% to 20%, it was found that the temperature rise of the focus was also gradually increased. Gajendra et al. also found that in five-layer of biological tissue, as the duty cycle of ultrasonic signal increased from 60% to 90%, the focal temperature also increased gradually [26]. Because the heat dose in the media was positively proportional to the duty cycle. In Figure 4 (c), the temperature rising at the focus decreased gradually with the increase of the inner radius of the transducer from 0.8 cm to 1.2 cm.

Discussion

Numerical simulations have shown that the optimal temperature distribution of a large angle concave spherical focused ultrasound transducer can be obtained by varying the operating parameters of the focused ultrasound transducer, such as frequency, duty cycle, and internal radius. To obtain optimal treatment, the temperature rise in tumor tissue should be high for irreversible tissue damage, while the temperature rise in healthy tissue should be relatively small to avoid unnecessary damage [27-29].

By changing the irradiation frequency, the biological tissue irradiated by large aperture concave spherical focused ultrasonic transducer was studied, and the relationship between the focal temperature rise and the frequency was analyzed. With the increase of frequency, the temperature in the focal region also increased gradually. In other words, when other parameters remain unchanged, and an increase in frequency enhanced the focusing ability of ultrasonic transducer. The effect of frequency on temperature rise depended on Q_v, which was correlated with the absorption coefficient and sound intensity. As the frequency increased, the absorption coefficient and sound intensity gradually increased, and the focal temperature also increased. The focal temperature of biological tissue reached a maximum when the contributions of the absorption coefficient and sound intensity to Q_v were balanced. However, when the frequency of ultrasonic transducer continues to increase, the contribution of sound intensity to Q_v will be better than the sound absorption coefficient, and the focal temperature of biological tissue will decrease [18,30,31]. This showed that the selection of appropriate ultrasonic transducer frequency was very important for the therapeutic effect of tumor. The effect of frequency on skin surface temperature rise can be ignored.

The higher the duty cycle, the greater the maximum temperature rise at the focal region of biological tissue, because higher duty cycles due to longer on time for the heat to be transferred to surrounding media, which can significantly increase the heat buildup in biological tissue through non-continuous energy deposition with higher temporal average intensity, and it was conducive to the absorption of energy by biological tissue, resulting in a significant increase in the temperature of focal region [32-34]. In order to obtain the best tumor treatment effect, the duty cycle of large aperture concave spherical focused ultrasound transducer can be adjusted to minimize the thermal damage to adjacent healthy tissue.

When the inner diameter of the focused ultrasound transducer increased, the maximum temperature rising in the focal region of biological tissue decreased. This was mainly because when the inner radius of the transducer increased, the surface acoustic energy decreased, which led to the decrease of the sound intensity at the focus, so the focal temperature decreased.

Conclusion

The distribution characteristics of HIFU sound field and temperature field corresponding to five-layer media irradiated by a large aperture concave spherical focused transducer under different frequency, duty cycle and inner diameter parameters were simulated. The effects of varied frequency, duty cycle and inner diameter parameters on temperature rise of five-layer media were discussed. The results showed that the maximum temperature rise increased with the increase of frequency and duty cycle. With the increase of the inner diameter of transducer, the maximum temperature rising of the tissue decreased gradually. Therefore, in actual HIFU treatment, it is very important to select appropriate frequency, duty cycle and inner diameter parameters, because they have an important impact on local temperature rise of tissue. This study can provide a theoretical basis for parameter optimization in HIFU treatment, and provide a theoretical reference for the temperature control of large aperture concave spherical focused ultrasound transducer in actual treatment of tumor tissue.

Acknowledgment

This work was supported by the Key Project of Hunan Provincial Department of Education of China under grant No. 21A0618, and the Changsha Natural Science Foundation Project under grant No. kq2202313.The authors sincerely thank the anonymous reviewers for their helpful comments and suggestions.

References

1. Xu D, Zou W, Luo Y, Gao X, Jiang B, Wang Y, et al. Feasibility between bifidobacteria targeting and changes in the acoustic environment of tumor tissue for synergistic HIFU. Scientific Reports. 2020 May 8;10(1):7772. DOI:10.1038/s41598-020-64661-6.
2. Ning G, Zhang X, Zhang Q, Wang Z, Liao H. Real-time and multimodality image-guided intelligent HIFU therapy for uterine fibroid. Theranostics. 2020; 10(10):4676-93. DOI:10.7150/ thno.42830.
3. Sazgarnia A, Shanei A, Taheri AR, Meibodi NT, Eshghi H, Attaran N, et al. Therapeutic effects of acoustic cavitation in the presence of gold nanoparticles on a colon tumor model. Journal of Ultrasound in Medicine. 2013 Mar;32(3):475-83. DOI:10.7863/ jum.2013.32.3.475.
4. Yuldashev PV, Karzova MM, Kreider W, Rosnitskiy PB, Sapozhnikov OA, Khokhlova VA.“HIFU Beam: ” A Simulator for Predicting Axially Symmetric Nonlinear Acoustic Fields Generated by Focused Transducers in a Layered Medium.IEEE Transactions on Ultrasonics, Ferroelectrics, and Frequency Control. 2021;68(9): 2837-52. DOI:10.1109/TUFFC.2021.3074611.
5. Zhao HM, Wang YL, Han FL, Ji YQ, Luo BW. Acoustic pressure simulation and experiment design in sea floor mining environment. Journal of Central South University. 2018; 25(6):1409-17. DOI:10.1007/s11771-018-3836-2.
6. Fan T, Chen T, Zhang W, Hu J, Zhang Y, Zhang D. Acoustic characterization of high intensity focused ultrasound field generated from a transmitter with large aperture. International Symposium on Therapeutic Ultrasound. 14th International Symposium on Therapeutic Ultrasound 2014. 2017; 1821:180002. DOI:10.1063/1.4977665.
7. Dong H, Gang L, Xin T. Influence of temperature-dependent acoustic and thermal parameters and nonlinear harmonics on the prediction of thermal lesion under HIFU ablation. Mathematical Biosciences and Engineering. 2021;18(2): 1340-51. DOI: 10.3934/mbe.2021070.
8. Haddadi S, Mohammad TA. Numerical and Experimental Evaluation of High-Intensity Focused Ultrasound-Induced Lesions in Liver Tissue Ex Vivo. Journal of Ultrasound in Medicine. 2018;37(6):1481-91. DOI:10.1002/jum.14491.
9. Kujawska T, Secomski W, Byra M, Postema M, Nowicki A. Annular phased array transducer for preclinical testing of anti-cancer drug efficacy on small animals. Ultrasonics. 2017 Apr 1;76:92-8. DOI:10.1016/ j.ultras. 2016.12.008.
10. Hudson TJ, Looi T, Pichardo S, Amaral J, Temple M, Drake JM, et al. Simulating thermal effects of MR-guided focused ultrasound in cortical bone and its surrounding tissue. Medical physics. 2018 Feb;45(2):506-19. DOI:10. 1002/mp. 12704.
11. Li Y, Tao C, Ma Q, Guo G, Zhang D, Hu J. Nonlinear acoustic-power measurement based on fundamental focal axial vibration velocity for high-intensity focused ultrasound. Journal of Applied Physics. 2018 Dec 7;124(21):214905. DOI:10.1063/1.5054665.
12. Lee KI. Measurement and numerical simulation of high intensity focused ultrasound field in water.Journal of the Korean Physical Society. 2017;71(10): 665-9. DOI:10.3938/jkps.71.665.
13. Andriyakhina YS, Karzova MM, Yuldashev PV, Khokhlova VA. Accelerated Thermal Ablation of Biological Tissue Volumes using HIFU beams with Shock Fronts. Acoustical Physics. 2019; 65(2):141-50. DOI:10.1134/S1063771019020015.
14. Sarkar R, Kumar Pandey P, Kundu S, Panigrahi PK. Exact sub and supersonic pressure wave-fronts in nonlinear thermofluid medium. Waves in Random and Complex Media. 2021 Jul 23:1-4. DOI:10.1080/ 17455030.2021.1954263.
15. Namakshenas P, Mojra A. Microstructure-based non-Fourier heat transfer modeling of HIFU treatment for thyroid cancer. Computer Methods and Programs in Biomedicine. 2020 Dec 1;197:105698. DOI:10.1016/j.cmpb.2020.105698.
16. Chang SH, Cao R, Zhang YB, Wang PG, Wu SJ, Qian YH, et al. Treatable focal region modulated by double excitation signal superimposition to realize platform temperature distribution during transcranial brain tumor therapy with high-intensity focused ultrasound. Chinese Physics B. 2018 Jul 1;27(7):078701. DOI:10. 1088/1674-1056/27/7/078701.
17. Gharloghi S, Gholami M, Haghparast A, Dehlaghi V. Numerical study for optimizing parameters of high-intensity focused ultrasound-induced thermal field during liver tumor ablation: HIFU Simulator.

Iranian journal of medical physics. 2017 Mar 1;14(1):15-22. DOI:10.22038/ijmp.2017. 19268. 1176.
18. Qi M, Liu J, Mao Y, Liu X. Temperature rise induced by an annular focused transducer with a wide aperture angle in multi-layer tissue. Chinese Physics B. 2018; 01(27):394-9. DOI: 10.1088/1674-1056/27/1/014301.
19. Li C, Chen S, Wang Q, Li H, Xiao S, Li F. Effects of thermal relaxation on temperature elevation in ex vivo tissues during high intensity focused ultrasound. IEEE Access. 2020 Nov 24;8:212013-21. DOI:10.1109/ACCESS. 2020.3040102.
20. Onal M, Esen A. A Crank-Nicolson Approximation for the time Fractional Burgers Equation. Applied Mathematics and Nonlinear Sciences. 2020;5(2):177-84. DOI:10.2478/amns. 2020.2. 00023
21. Wang D, Li L, Ji Y, Yan Y. Model recovery for Hammerstein systems using the auxiliary model based orthogonal matching pursuit method. Applied Mathematical Modelling. 2018 Feb 1;54:537-50. DOI:10.1016/j.apm.2017.10.005.
22. Guo C C, Ren Q F, Wan X L.The Research of Nonlinear Characteristics of High Intensity Focused Ultrasound in Biological Tissue.2020 5th International Conference on Mechanical, Control and Computer Engineering (ICMCCE), IEEE. 2020;418-21. DOI:10.1109/ ICMCCE51767. 2020.00098.
23. Gupta P, Atul S. Numerical analysis of thermal response of tissues subjected to high intensity focused ultrasound. International Journal of Hyperthermia. 2018; 35(1): 419-34. DOI:10.1080/ 02656736.2018.1506166.
24. Wang M, Zhou Y. High-intensity focused ultrasound (HIFU) ablation by frequency chirp excitation: Reduction of the grating lobe in axial focus shifting. Journal of Physics D: Applied Physics. 2018; 51(28): 285402. DOI:10.1088/1361-6463/aacaed.
25. Brás T, Paulino AF, Neves LA, Crespo JG, Duarte MF. Ultrasound assisted extraction of cynaropicrin from Cynara cardunculus leaves: Optimization using the response surface methodology and the effect of pulse mode. Industrial crops and products. 2020 Aug 1;150:112395. DOI:10.1016/j.indcrop. 2020. 112395.
26. Singh G, Paul A, Shekhar H, Paul A. Pulsed ultrasound assisted thermo-therapy for subsurface tumor ablation: a numerical investigation. Journal of Thermal Science and Engineering Applications. 2021 Aug 1;13(4). DOI:10.1115/1.4048674.
27. Suomi V, Jaros J, Treeby B, Cleveland RO. Full modeling of high-intensity focused ultrasound and thermal heating in the kidney using realistic patient models. IEEE Transactions on Biomedical Engineering. 2017 Jul 28;65(5):969-79. DOI:10.1109/TBME.2017.2732684.
28. Li X, Lovell JF, Yoon J, Chen X. Clinical development and potential of photothermal and photodynamic therapies for cancer. Nature reviews Clinical oncology. 2020 Nov;17(11):657-74. DOI: 10.1038/s41571-020-0410-2.
29. Amir A, Mojra A, Ashrafizadeh A. A numerical study on thermal ablation of brain tumor with intraoperative focused ultrasound.Journal of thermal biology. 2019;83:119-33. DOI:10.1016/j. jtherbio.2019.05.019.
30. Sadeghi-Goughari Moslem,Jeon S,Kwon H J. Analytical and Numerical Model of High Intensity Focused Ultrasound Enhanced With Nanoparticles. IEEE Transactions on Biomedical Engineering. 2020; 67(11): 3083-93. DOI: 10.1109/TBME.2020.2975746.
31. Kim H, Wu H, Cho N, Zhong P, Mahmood K, Lyerly HK, et al. Miniaturized intracavitary forward-looking ultrasound transducer for tissue ablation.IEEE Transactions on Biomedical Engineering. 2019;67(7):2084-93. DOI:10.1109/TBME.2019.2954524.
32. Qiao Y, Yin H, Chang N, Wan M. Phase-shift nano-emulsions induced cavitation and ablation during high intensity focused ultrasound exposure. International Symposium on Therapeutic Ultrasound. 14th International Symposium on Therapeutic Ultrasound. 2017; 1821(1):040001-1. DOI: 10.1063/1.4977617.
33. Tu J, Ha Hwang J, Chen T, Fan T, Guo X, Crum LA, et al. Controllable in vivo hyperthermia effect induced by pulsed high intensity focused ultrasound with low duty cycles. Applied physics letters. 2012 Sep 17;101(12):124102. DOI:10.1063/1.4754113.
34. Peng S, Zhou P, He W, Liao M, Chen L, Ma CM. Treatment of hepatic tumors by thermal versus mechanical effects of pulsed high intensity focused ultrasound in vivo. Physics in Medicine & Biology. 2016 Aug 31;61(18):6754. DOI:10.1088/0031-9155/61/18/6754.